Environmental Health Engineering and Management Journal 2024, 11(3), 273-284
http://ehemj.com
doi 10.34172/EHEM.2024.27

Environmental Health Engineering and Management Journal

Original Article

Environmental Health Engineering and Management

Open Access Publish Free

Congo red dye adsorption on dry green pea husk: Effects of process parameters and modeling approaches

Khaled Muftah Elsherif[1*], Abdulfattah Mohammed Alkherraz[2], Howell Edwards[3], Basma Younus Abdulsalam Mutawia[2]

[1]Libyan Authority for Scientific Research, Tripoli, Libya
[2]Chemistry Department, Faculty of Science, Misurata University, Misurata, Libya
[3]School of Chemistry and Bioscience, Faculty of Life Sciences, University of Bradford, UK

Abstract

Background: Congo red (CR), a harmful dye present in water, requires effective removal methods. This study investigated the utilization of dry green pea husk (DGPH) and its charcoal (CGPH) as economical and eco-friendly adsorbents.

Methods: Various factors, including contact time, pH, adsorbent dosage, initial concentration, and temperature, were investigated to assess their impact on the adsorption process. Also, different models (isotherms, kinetics, and thermodynamics) were compared to describe the adsorption phenomenon.

Results: Equilibrium adsorption was achieved within 30 minutes for both adsorbents. The optimum pH for CR removal was determined to be 2. The adsorption capacity decreased by increasing the adsorbent dosage, whereas it increased by increasing the initial dye concentration. The Langmuir isotherm model demonstrated the best fit for DGPH, while the Freundlich model exhibited the best fit for CGPH. The pseudo-second-order model displayed a superior fit for both adsorbents. To assess the spontaneity and feasibility of the adsorption process, thermodynamic parameters including enthalpy, entropy, and Gibbs free energy were computed. The results indicated that the adsorption of CR on DGPH was endothermic and favorable at lower temperatures, whereas the adsorption on CGPH was exothermic and favorable at higher temperatures. The negative values of Gibbs free energy for the CGPH adsorbent confirmed the spontaneous nature of the adsorption process.

Conclusion: The study establishes that green pea husk and its charcoal are effective and environmentally friendly alternatives for the removal of CR from water.

Keywords: Congo red, Adsorption, Charcoal, Kinetics, Thermodynamics

Citation: Elsherif KM, Alkherraz AM, Edwards H, Mutawia BYA. Congo red dye adsorption on dry green pea husk: Effects of process parameters and modeling approaches. Environmental Health Engineering and Management Journal 2024; 11(3): 273-284 doi: 10.34172/EHEM.2024.27.

Article History:
Received: 17 November 2023
Accepted: 18 May 2024
ePublished: 28 June 2024

***Correspondence to:**
Khaled Muftah Elsherif,
Email: elsherif27@yahoo.com

Introduction

Synthetic dyes are widely used in various industries such as textiles, leather, cosmetics, paper, printing, and plastics (1). However, they cause serious environmental problems when they are discharged into water bodies. They reduce the sunlight penetration and the photosynthetic activity of aquatic plants. They also increase the organic load of water, disrupting the ecological balance of aquatic life (2). Moreover, synthetic dyes are harmful to human health because they have mutagenic and carcinogenic effects (3). Therefore, it is essential to treat the wastewater before releasing it into the environment to avoid these risks (4).

One of the main types of synthetic colorants is azo dyes (e.g., Congo red), which are preferred in the textile industry for their variety of shades, color fastness, and low energy consumption (5). However, excessive use of azo dyes generates a large amount of wastewater containing azo dye pollutants (6). Congo red (CR), a diazo dye, is classified as a carcinogen because it contains an aromatic amine in its chemical composition. Azo dyes are resistant to natural degradation because of their aromatic nature. They persist in the environment for extended periods and have a detrimental impact on the locals. This technology offers several advantages, including its ability to effectively manage large amounts of wastewater and produce outputs of exceptional quality (7). Various treatment methods have been proposed and applied for this kind of wastewater, such as ion exchange resin, biodegradation, electrocoagulation, coagulation-flocculation, membrane filtration, photocatalysis, Fenton oxidation, ozonation, and adsorption (8-14). However, several of these methods present certain drawbacks, such as the inhibition of bacterial growth, the production of sludge, unsuitability for certain colors, limited lifespan,

high costs, slow reaction rates, and the generation of byproducts (15). Therefore, in recent years, researchers have focused on adsorption technology for dye removal (16). This technology offers various advantages, including its capacity to efficiently manage substantial quantities of wastewater and deliver outputs of exceptional quality (17).

Adsorption is widely recognized as a highly efficient wastewater treatment technique due to its cost-effectiveness, simplicity, and effectiveness (18). The dye cannot be easily degraded by biodegradation; hence, it must be adsorbed to prevent its discharge into the environment. Many researchers have investigated various adsorbent materials in search of the best one for dye treatment, such as carbon-based materials (19), silica composites, cellulosic materials, and chitosan-related compounds (19-22). Natural and low-cost adsorbents such as tea waste, orange peel, and beech wood sawdust have also been investigated (23-25).

This study examined the removal of CR from aqueous solution using dry green pea husk (DGPH) and green pea husk charcoal (CGPH). The adsorption isotherm behavior of CR on DGPH and CGPH was evaluated using experimental and modeling methods. The adsorption of CR was studied using kinetic, isotherm, and thermodynamic adsorption models. Furthermore, this study investigated the effects of adsorbent dosage, contact time, pH, initial dye concentration, and temperature on the CR adsorption capacity.

Materials and Methods

Preparation of adsorbent material

The green pea husks were obtained from supermarkets in the Misurata region and underwent a thorough washing process with tap water to remove water-soluble impurities and foreign particles. Afterward, the biomass was sun-dried for two weeks, finely ground, and subjected to multiple rinses using distilled water. The resulting material was then dried in an oven at 60 °C for 48 hours. To attain particle sizes ranging from 200 to 250 μm, the biomass adsorbent material, which had been dried and pulverized, underwent sieving using a sieve conforming to the American Society for Testing and Materials (ASTM) standard. This particular adsorbent material was identified as "DGPH".

Fifty grams of powdered adsorbent was accurately weighed and transferred into crucibles. Subsequently, the sample underwent carbonization at a temperature of 550 °C for 1 hour. The resulting adsorbent material was thoroughly rinsed and dried following the carbonization process. The designation "CGPH" was assigned to this particular adsorbent substance.

Chemicals

CR, a specific azo dye with a molecular formula of $C_{32}H_{22}N_6Na_2O_6S_2$ and a molecular weight of 696.7 g/mol, was provided by Sigma-Aldrich. HCl and NaOH were also provided by Sigma-Aldrich and used without further purification. To adjust the pH, 0.1 M NaOH or 0.1 M HCl solutions were employed. All chemicals used in this study were of analytical grade. Dye solutions with concentrations ranging from 1 to 300 mg/L were prepared by diluting a stock solution of CR (500 mg/L) with distilled water.

Adsorption procedure

The batch process methods were used to evaluate the CR adsorption on DGPH and CGPH. The present study investigated the impact of key experimental variables on the adsorption process, employing batch experiments according to the methodology outlined by Elsherif et al (10). This research explored the effects of pH, contact time, dose, temperature, and initial metal ion concentrations. The experimental conditions are shown in Table 1. Each experiment utilized a 50 mL dye solution containing an initial concentration of CR at 50 mg/L. The solution was added to 100 mL conical flasks, along with the required amount of adsorbent. The samples (dye and adsorbent) were then shaken continuously at a constant speed of 175 rpm and a constant temperature of 25 °C.

To determine the optimal pH for maximum CR adsorption, both DGPH and CGPH adsorbents were used. Each experimental trial involved combining a 50 mL solution containing 50 mg/L of CR with 0.1 g of OSP in 150 mL Erlenmeyer flasks. The initial pH of the solution ranged from 3 to 13. The mixtures were then agitated at 175 rpm for 30 minutes at a temperature of 25 ± 1 °C. Once equilibrium was reached, the final pH of each combination was measured and recorded. The samples were filtered, and the concentrations of the filtrates were subsequently determined.

To examine the impact of adsorbent dosage, a series of 100 mL Erlenmeyer flasks were prepared. Each flask was filled with 50 mL of dye solution, which had a concentration of 50 mg/L. Varying quantities of biosorbent, ranging from 0.1 to 3.5 g, were then introduced into each flask. The mixtures were subsequently agitated using a shaker, operating at a speed of 175 rpm for 30 minutes. Throughout this process, the temperature was maintained at 25 ± 1 °C, and the pH level was optimized based on the results from a prior experiment. Following

Table 1. Variation of operating conditions for adsorption experiments

Experimental parameters	Interval value
Contact time	0-60 min
pH	3.0-13.0
Initial concentration	1.0-300.0 mg/L
Adsorbent dosage	0.1-3.5 g
Temperature	25.0-60.0 °C

agitation, the mixtures were filtered, and the remaining metal ions were subjected to analysis.

To investigate the contact time, the adsorption experiments were carried out using a series of Erlenmeyer flasks. Each flask was filled with 0.1 g of biosorbent and 50 mL of a dye solution with a concentration of 50 mg/L. The solutions were then agitated in a water bath, maintaining a controlled temperature of 25 ± 1 °C and an agitation rate of 175 rpm, while also ensuring the pH was optimized. Samples were collected periodically at regular intervals (0-60 minutes) to monitor the advancement of the adsorption process.

Under optimized conditions, the influence of initial metal ion concentrations on adsorption was examined. To accomplish this, 0.1 g of each adsorbent was mixed with 50 mL of dye solutions with initial concentrations varying from 1.0 to 300.0 mg/L, while keeping the pH at an optimized level. The experiments were carried out for 30 minutes at a constant temperature of 25 ± 1 °C and a shaking rate of 175 rpm. Following that, the samples were filtered, and the remaining metal ions were quantified using an atomic absorption spectrophotometer.

The concentrations of CR before and after adsorption were determined using a UV/visible spectrometer (Jenway 6305 UV-VIS) at a wavelength of 490 nm (26). To estimate the CR removal efficiency, the following calculation (27) was employed:

$$\%R = \frac{(C_o - C_e)}{C_o} x100 \quad (1)$$

The CR adsorption capacity was determined using the following equation (27):

$$Q_e = \frac{(C_o - C_e) x V}{M} \quad (2)$$

In the given equations, C_o (mg/L), C_e (mg/L), V (L), and M (g) denote the initial concentration of CR, the equilibrium concentration of CR, the volume of the aqueous solution, and the mass of the dry adsorbent, respectively.

Results

Influence of pH

The effect of pH on CR dye adsorption capacity using DGPH and CGPH is shown in Figure 1a. It can be seen that acidic pH values have a significant influence on the CR removal efficiency. The adsorption efficiency of the adsorbents decreased as the pH increased from 2 to 12. The maximum adsorption of CR dye was achieved at a pH of 2, with removal percentages of 89.0% for DGPH and 99.8% for CGPH. Therefore, pH 2 was chosen for further experiments.

Adsorbent dosage effect

The effect of adsorbent dose on the adsorption capacity of CR dye is illustrated in Figure 1b. It can be observed that the adsorption capacity decreased as the adsorbent dose increased. For instance, when the adsorbent weight increased from 0.1 to 3.5 g, the equilibrium adsorption capacity of CR dye decreased from 19.3 to 0.6 mg/g for DGPH and from 23.2 to 0.7 mg/g for CGPH. Therefore, a 0.1 g adsorbent dose was selected as the optimal value for

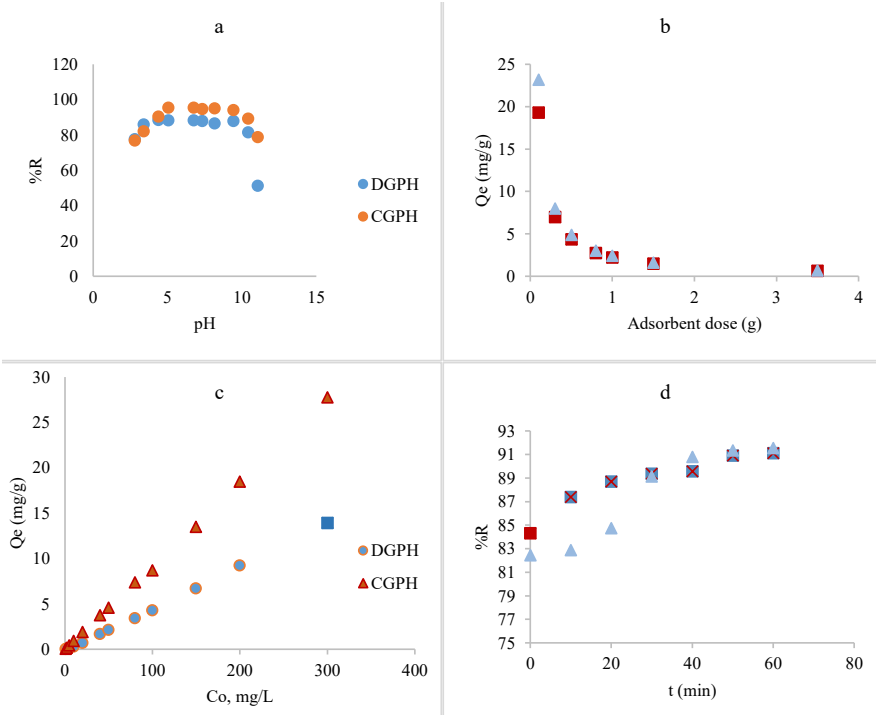

Figure 1. Effect of process parameters on adsorption efficiency onto DGPH and CGPH: a) pH, b) adsorbent dose, c) initial concentration, d) contact time

the adsorption of CR onto both adsorbents.

Initial concentration effect

Figure 1c depicts the effects of the initial dye concentration on the removal of CR. As the initial dye concentrations ranged from 1 to 300 mg/L, the amount of dye adsorbed at equilibrium displayed an ascending trend, reaching values of 0.03 to 13.9 mg/g for DGPH and 0.08 to 27.8 mg/g for CGPH. These results indicate that there are still available adsorbent sites for adsorption, and saturation has not been reached yet.

To evaluate the effectiveness of DGPH and CGPH adsorbents in removing CR dye from water solutions, the suitability of adsorption was assessed using several isotherm models, including Langmuir, Freundlich, Temkin, Dubinin-Radushkevitch, and Jovanovic. These models were utilized to analyze the adsorption process and understand the adsorption behavior of the adsorbents towards CR dye.

The Langmuir adsorption isotherm model describes the adsorption of a single layer of adsorbate on the external surface of the adsorbent, beyond which no further adsorption takes place. This model assumes that the adsorption surface is uniform and consists of a fixed number of equivalent sites. It also considers the adsorption energy to be constant and independent of the surface coverage and assumes that the adsorbate does not undergo lateral movement on the surface plane (16). The linear form of the Langmuir equation is expressed as Eq. (3):

$$\frac{1}{Q_e}=\frac{1}{Q_m}+\frac{1}{b\,Q_m\,C_e} \quad (3)$$

Qm, *b*, and *Ce* represent the maximum amount of adsorbate per unit mass of adsorbent, the affinity of the adsorbent for the adsorbate, and the adsorbate concentration in the solution at equilibrium, respectively. Moreover, the Langmuir model parameter R_L, which indicates the type of adsorption isotherm, can be calculated by the following formula (16):

$$R_L=\frac{1}{1+b\,C_o} \quad (4)$$

The Langmuir model is associated with the equilibrium parameter R_L, which has no units. The symbols C_o and *b* stand for the equilibrium concentrations of the dye and the Langmuir constant, respectively. The type of adsorption depends on the value of R_L: $R_L = 0$ means the adsorption is irreversible, $0 < R_L < 1$ means the adsorption is favorable, and $R_L > 1$ means the adsorption is unfavorable (16).

The Langmuir isotherm constants, Q_m and K_L, which represent the maximum adsorption capacity and the adsorption affinity, respectively, can be determined by analyzing the graph of $1/Q_e$ versus $1/C_e$ at room temperature (Figure 2a). The slope of the linear plot corresponds to $1/b.Q_m$, while the intercept gives $1/ Q_m$. By calculating these values from the graph, the Langmuir constants Q_m and K_L can be obtained, providing insights into the adsorption capacity and affinity of the adsorbent for the given system.

The Freundlich adsorption isotherm describes the relationship between the surface diversity and the exponential variation of active sites and their energies. The Freundlich equation in its linear form is as follows (28):

$$\mathrm{Log}Q_e=\mathrm{Log}K_f+\frac{1}{n}\,\mathrm{Log}C_e \quad (5)$$

The Freundlich equation has two parameters: K_f, which indicates the strength of the bond between the adsorbate and the adsorbent, and *1/n*, which measures the extent of non-linearity in the adsorption process. The graph of $\log Q_e$ versus $\log C_e$ (shown in Figure 2b) is linear. The intercept and slope give the Freundlich isotherm constants, K_f and n, which describe the adsorbent-adsorbate system. A favorable adsorption process occurs when n is between one and ten (28).

Temkin isotherm model considers the effects of indirect adsorbent/adsorbate interactions on the adsorption process; it also implies that the adsorption heat (temperature-dependent) of all molecules in the layer declines linearly as the surface coverage increases because of adsorbent–adsorbate interactions. The equation in its linear form is as follows (29):

$$Q_e=B\,\mathrm{Log}\,A+B\,\mathrm{Log}C_e \quad (6)$$

The highest binding energy is represented by the equilibrium binding constant A, and the constant B is associated with the biosorption heat. The slope and intercept of the graph of Q_e against $\log C_e$ can be used to calculate the isotherm constants A and B. The Temkin isotherm is presented in Figure 2c.

The adsorption mechanism involving a heterogeneous surface and a Gaussian energy distribution is commonly characterized by the Dubinin–Kaganer–Radushkevich (DKR) isotherm. This model has demonstrated good agreement with experimental data in cases of high solute activities and within a moderate concentration range (30). The linear form of the DKR isotherm, represented by equation (7), is as follows:

$$\mathrm{Log}Q_e=\mathrm{Log}Q_d+\beta\varepsilon^2 \quad (7)$$

The free energy is associated with the DKR isotherm constant β and the isotherm saturation capacity Q_m is theoretical. The slope and intercept of the graph of log Q_e against ε^2 can be used to find the DKR isotherm parameters β and Q_d, which describe the adsorption mechanism with a Gaussian energy distribution on a

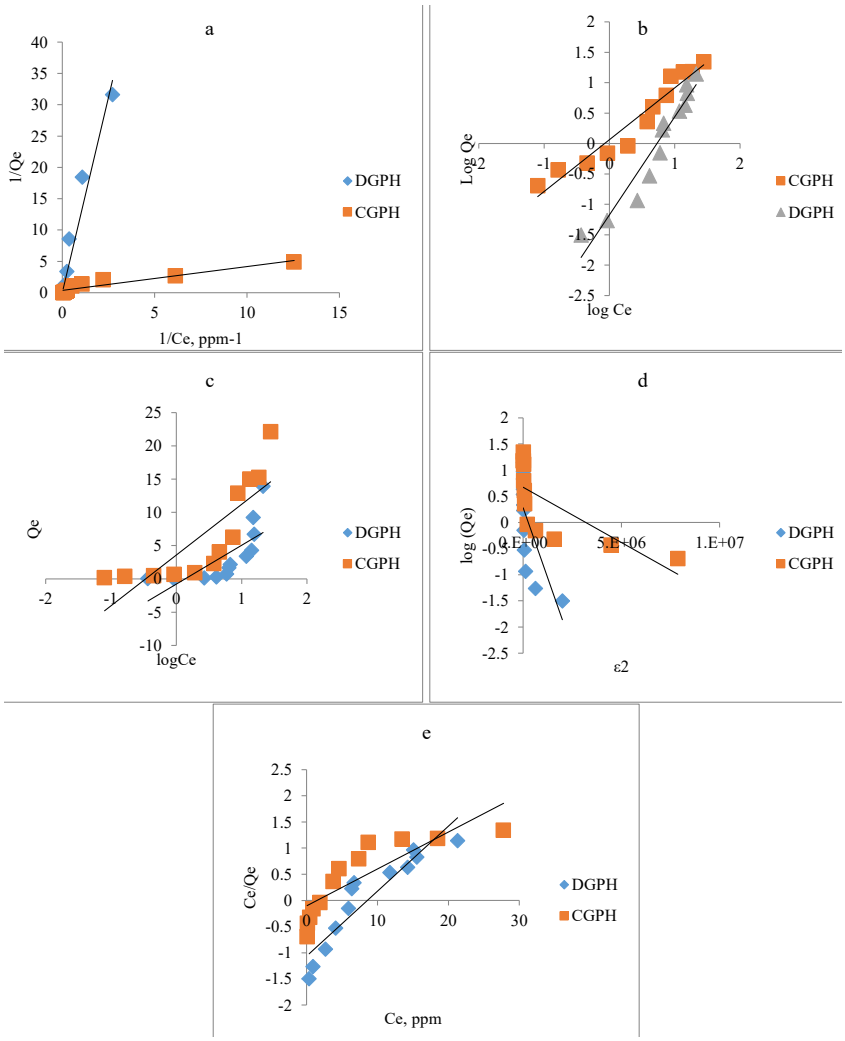

Figure 2. Isotherm model plots for adsorption of CR onto DGPH and CGPH: a) Langmuir, b) Freundlich, c) Temkin, d) DKR, e) Jovanovic

heterogeneous surface (Figure 2d). The value of ε (Polanyi potential) is connected to C_e (mg/L) by the Equation (30):

$$\varepsilon = \mathrm{RT\ Log}\left(1+\frac{1}{C_e}\right) (8)$$

Also, the mean free energy € for each adsorbate molecule is calculated using the following equation:

$$E = \frac{1}{\sqrt{2\beta}} (9)$$

The Jovanovic isotherm model extends the assumptions of the Langmuir model by considering the possibility of mechanical interactions between the adsorbate and the adsorbent. This model takes into account additional effects beyond simple adsorption and incorporates the influence of these mechanical interactions. The linear equation representing the Jovanovic isotherm model can be found in references (31):

$$\mathrm{Log\ Q_e = Log}\ Q_m + S_J C_e (10)$$

The variables Q_e, Q_m, and S_J represent the amount of adsorbate adsorbed, the maximum adsorption capacity according to the Jovanovic model, and the Jovanovic isotherm constant, respectively. The values of S_J and Q_m were obtained by analyzing the slope and intercept of a linear graph plotting log Q_e against C_e. The Jovanovic isotherm model is shown in Figure 2e. Table 2 presents the parameters of various isotherm models utilized in this study at a temperature of 25 °C.

Contact time effect

This research aimed to determine the time required for the adsorption process to reach equilibrium. The impact of time was examined under specific conditions: the pH of the solution remained unaltered, the temperature was maintained at room temperature, the concentration of CR was fixed at 50 mg/L, and both adsorbent materials (DGPH and CGPH) were used in equal masses of 0.1 g each. Figure 1d illustrates the time variation ranging from 0 to 60 minutes. The findings indicate that the adsorption process attained equilibrium within 30 minutes.

The adsorption kinetics of CR on DGPH and CGPH adsorbents were investigated at a temperature of 25 °C.

Table 2. Langmuir, Freundlich, Temkin, Dubinin-Radushkevich, and Jovanovic isotherm model parameters for CR adsorption onto DGPH and CGPH adsorbents

Langmuir	Q_m (mg/g)	b (L/mg)	R_L	R^2
DGPH	45.25	0.002	0.917	0.9526
CGPH	2.69	0.978	0.276	0.9155
Freundlich	**K_f (mg/g (L/mg)$^{1/n}$)**	**n (g/L)**	**R^2**	
DGPH	14.90	0.62	0.9262	
CGPH	1.16	1.17	0.9390	
Temkin	**A (L/mg)**	**B (J/mol)**	**R^2**	
DGPH	1.36	5.84	0.5052	
CGPH	2.96	7.63	0.6770	
DKR Model	**Q_d (mol/g)**	**β (mol^2/J^2)**	**E (kJ/mol)**	**R^2**
DGPH	1.92	1.0x10^{-6}	0.707	0.4841
CGPH	4.72	0.2x10^{-6}	1.581	0.5185
Jovanovic	**Q_m (mg/g)**	**S_J (L/g)**	**R^2**	
DGPH	11.64	0.124	0.8631	
CGPH	1.27	0.071	0.7184	

Various models, such as pseudo-first-order, pseudo-second-order, Elovich, and intraparticle diffusion models (32,33), were used to calculate the rate constants. The kinetic curves for CR adsorption on DGPH and CGPH are shown in Figures 3a, 3b, 3c, and 3d, and the relevant kinetic parameters are listed in Table 3.

The pseudo-first-order model, represented by equation (11), assumes that the rate of change of CR adsorption over time is influenced by the difference between Q_e and Q_t, where Q_e (mg/g) refers to the amount of CR adsorbed at equilibrium and Q_t (mg/g) represents the amount of CR adsorbed at a given time (23):

$$\log(Q_e - Q_t) = \log(Q_e) - \frac{k_1}{2.303} \times t \quad (11)$$

The pseudo-first-order adsorption rate constant, denoted as k_1 (min^{-1}), is determined based on the time variable *t*. A linear graph of log (Q_e – Q_t) against *t* confirms the suitability of this kinetic model, as illustrated in Figure 3a. The intercept and slope of the graph can be used to calculate the values of Q_e and k_1, respectively. The recorded values of the rate constant (k_1) for the adsorption of CR onto DGPH and CGPH can be found in Table 3.

Equation (12) represents the linearized expression for the pseudo-second-order kinetic model, as described in previous studies (23,27,34)

$$\frac{t}{Q_t} = \frac{1}{k_2 \times Q_e^2} + \frac{t}{Q_e} \quad (12)$$

The second-order adsorption rate constant, represented as k_2 (g/mg·min), is determined by considering the equilibrium adsorbed amount Q_e and the adsorbed amount Q_t of CR at any given time (t), both measured in mg/g. The pseudo-second-order kinetic parameters were obtained by plotting (t/Q_t) against t, as shown in Figure 3b, and the corresponding values are presented in Table 3. These parameters provide insights into the rate of adsorption and the interaction between the adsorbate and adsorbent in the system.

For the Elovich kinetic model, equation (13) (34) represents the linear form:

$$Q_t = \frac{1}{\beta}\ln(a\beta) + \frac{1}{\beta}\ln(t) \quad (13)$$

In the Elovich model, the parameter α (mg·g^{-1}·min^{-1}) corresponds to the initial adsorption rate, while the parameter b (g·mg^{-1}) is associated with the experiment-specific desorption constant. The Elovich model kinetic parameters were derived from the plot of (Q_t) versus ln(t) (Figure 3c), and are presented in Table 3.

The intraparticle diffusion model is a relationship that is empirically specific and can be represented as follows (32):

$$Q_t = K_{id} t^{1/2} + C \quad (14)$$

The rate constant, represented by K_{id}, is a significant parameter in the intraparticle diffusion model. The C values correspond to the thickness of the boundary layer, with a higher intercept value indicating a more efficient boundary layer (32). This model is applicable for describing various adsorption processes in which the adsorbed molecules exhibit a nearly proportional relationship with $t^{1/2}$. As per Equation (14), plotting Q_t against $t^{1/2}$ yields a linear graph with the slope representing K_{id} and the intercept representing C. This analysis assumes that the adsorption mechanism follows the phenomena of intraparticle diffusion. The intraparticle diffusion model kinetic parameters were derived from the plot of (Q_t) versus $t^{1/2}$ (Figure 3d) and are presented in Table 3.

Temperature effect

In this study, the impact of temperature on dye adsorption on DGPH and CGPH was investigated. The adsorption capacity was evaluated at various temperatures, including 298, 303, 308, 313, 318, 323, and 333 K. Figure 4 shows distinct behaviors for DGPH and CGPH. Specifically, the adsorption capacity of DGPH increased with temperature, while the adsorption capacity of CGPH decreased with temperature. The dye adsorption capacity for DGPH exhibited an increase from 2.17 to 2.33 mg/g, whereas for CGPH, it decreased from 4.60 to 4.10 mg/g as the temperature ranged from 298 to 333 K. These results suggest that the adsorption process of DGPH is endothermic, while that of CGPH is exothermic.

The effect of temperature on adsorption capacity is illustrated in Figure 4. The adsorption capacity of DGPH increases with temperature because the higher temperature provides more energy for the adsorption reaction to overcome the activation energy barrier. The

Table 3. Kinetic parameters for CR adsorption onto DGPH and CGPH

Pseudo-first-order	**k_1 (min^{-1})**	**Q_e (Est.) (mg/g)**	**Q_e (Exp.) (mg/g)**	**R^2**
DGPH	0.006	2.88	2.25	0.785
CGPH	0.037	1.79	4.50	0.915
Pseudo-second-order	**k_2 ($g.mg^{-1}.min^{-1}$)**	**Q_e (Est.) (mg/g)**	**Q_e (Exp.) (mg/g)**	**R^2**
DGPH	2.235	2.25	2.25	1.0000
CGPH	0.289	4.57	4.50	0.9995
Elovich	**B ($g.mg^{-1}$)**	**A ($mg.g^{-1}.min^{-1}$)**		**R^2**
DGPH	12.27	$5.97x10^{24}$		0.9936
CGPH	3.98	$2.98x10^{15}$		0.7255
Intra-particle diffusion	**K_{id} ($mg.g^{-1}.min^{-1}$)**	**C (mg/g)**	**Q_e (Exp.) (mg/g)**	**R^2**
DGPH	0.018	2.12	2.25	0.9443
CGPH	0.063	4.05	4.50	0.8413

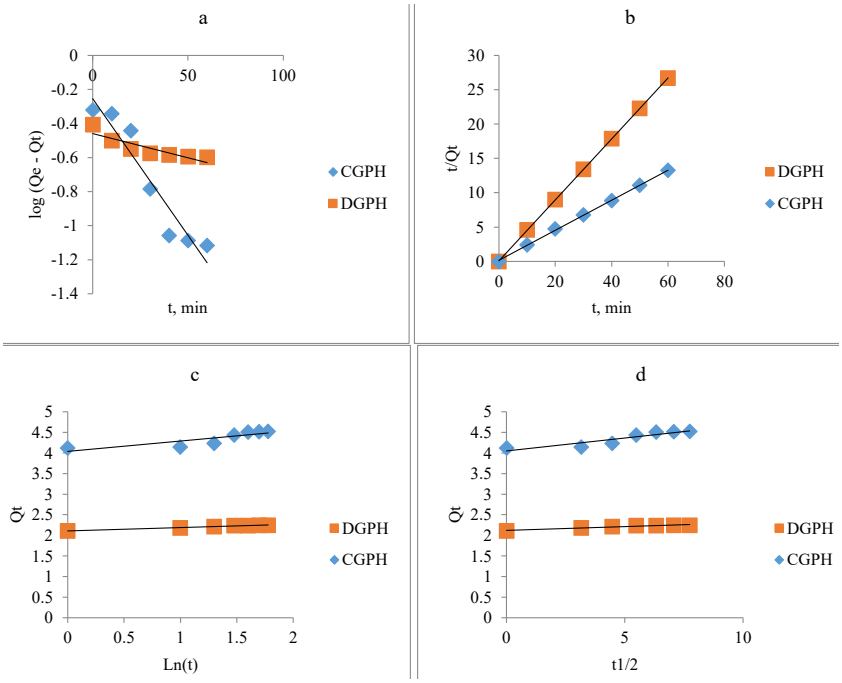

Figure 3. Kinetic graph for the adsorption of CR onto DGPH and CGPH: a) Pseudo-First-Order, b) Pseudo-Second-Order, c) Elovich, d) Intraparticle diffusion

adsorption capacity of CGPH decreases with temperature because the higher temperature reduces the attraction between the adsorbent and the adsorbate, and promotes the desorption reaction. The thermodynamic parameters, such as the standard Gibbs free energy change (ΔG^o), standard enthalpy change (ΔH^o), and standard entropy change (ΔS^o), were calculated using the following equations (28,29,35):

$$K_d = \frac{Q_e}{C_e} \quad (15)$$

$$\Delta G^o = \Delta H^o - T\,\Delta S^o \quad (16)$$

$$\Delta G^o = -RT\,\mathrm{Ln}\,K_d \quad (17)$$

$$\mathrm{Ln}K_d = \frac{\Delta S^o}{R} - \frac{\Delta H^o}{RT} \quad (18)$$

Several parameters are involved in the equations including the universal gas constant R (8.314 J/K.mol), the absolute temperature T (K), the equilibrium dissociation constant K_d (L/g), and the equilibrium values of the dye concentration in solution C_e (mg/L), and the dye amount adsorbed onto the adsorbent Q_e (mg/g).

To determine the values of ΔH^o and ΔS^o, equation (18) was used to analyze the linear relationship between ln (K_d) and 1/T (28,29), as shown in Figure 5. Table 4 summarizes the thermodynamic parameters obtained for the adsorption process.

Discussion

Influence of process parameters on the adsorption phenomenon

The investigation of contact time, as depicted in Figure 1d, demonstrated a progressive increase in the percentage of

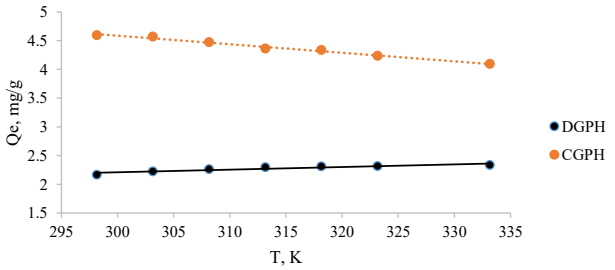

Figure 4. Effect of temperature on adsorption capacity of CR onto DGPH and CGPH

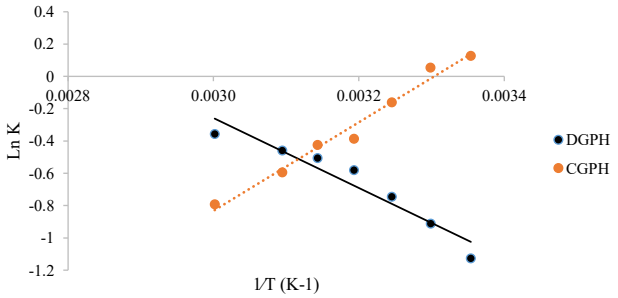

Figure 5. Thermodynamic study of CR adsorption onto DGPH and CGPH

dye removal with prolonged contact time. A substantial clearance rate was initially observed due to the large surface area available for dye adsorption. However, over time, the adsorbent's capacity diminished rapidly, resulting in challenges in occupying the remaining unoccupied surface sites. This can be attributed to repulsive interactions between solute molecules present in the solid and bulk phases. Based on the analysis of these findings, an equilibrium point of 30 minutes was determined in the batch adsorption experiments. These results align with the results of previous literature reports on dye removal (36).

The solution pH can affect the surface properties of the adsorbent and the ionization state of the adsorbate (37). The adsorption of $H^+$and OH^- ions in the solution, which depends on the solution pH, also, influences the adsorption of the adsorbate (38). In this study, as shown in Figure 1a, the optimal pH value was found to be 2. This can be explained by the changes in the surface charge of the adsorbents. By reducing the initial pH, the positive charges on the adsorbent surface increased, leading to a higher adsorption capacity at more acidic pH values. On the other hand, electrostatic repulsions between the negatively charged adsorbents and CR increased at alkaline pH values (39).

The adsorbent dose is an important factor in the adsorption process because it determines the equilibrium between the adsorbent and the adsorbate in the system. It can also be used to estimate the cost of adsorbent treatment per unit of dye solution (40). As shown in Figure 1b, the adsorbed amount of CR decreased as the adsorbent dose increased. This decrease in adsorption capacity can be attributed to the overlapping or aggregation of active sites as the dosage increases, making the sites inaccessible for the dye. Similar results have been reported in previous studies (34).

The initial dye concentration plays a crucial role in generating the required driving force to overcome resistance during the mass transfer of dye molecules between the aqueous and solid phases. In this study, as illustrated in Figure 1c, it was observed that the amount of CR adsorbed increased with the initial concentration. This effect can be attributed to the heightened driving force resulting from an augmented concentration gradient caused by an increase in the initial dye concentration (41,42). Moreover, higher initial dye concentrations enhance the interaction between CR and the adsorbent, thereby promoting increased CR adsorption.

Table 4. Thermodynamic properties of CR dye adsorption on adsorbents at 25°C

Adsorbed Surface	ΔG° (kJ.mol^{-1})	ΔH° (kJ.mol^{-1})	ΔS° (kJ.mol^{-1})	R^2
DGPH	2.550	18.01	0.0519	0.9231
CGPH	-0.351	-22.79	-0.0753	0.9798

Adsorbent isotherms

At a temperature of 25 °C, the parameters of different isotherm models employed in this study are presented in Table 2. The models evaluated include Langmuir, Freundlich, Temkin, Dubinin–Radushkevich, and Jovanovic. The selection of the most suitable model was based on identifying the R^2 value that is closest to 1. By comparing the goodness-of-fit of these models, the one with the highest R^2 value was considered the most appropriate for describing the adsorption behavior in this investigation.

The suitability of different models for the adsorption process was assessed based on the R^2 value. For DGPH, the results showed that Langmuir ($R^2=0.9526$) had the highest fit, followed by Freundlich ($R^2=0.9262$), Jovanovic ($R^2=0.8631$), Temkin ($R^2=0.5052$), and DKR ($R^2=0.4841$), respectively. These results indicate that the adsorption process follows the formation of a monolayer of adsorbate on the outer surface of the adsorbent, beyond which no further adsorption takes place. The Langmuir equation allows calculating the dimensionless separation factor (R_L). The R_L value was 0.917. This implies that the DGPH adsorbed CR favorably. The maximum adsorption capacity of CR onto DGPH, as calculated from the Langmuir equation, was found to be 45.25 mg/g at a temperature of 25°C.

The adsorption of CR onto CGPH was better fitted by the Freundlich model ($R^2=0.9390$), followed by the Langmuir ($R^2=0.9155$), Jovanovic ($R^2=0.7184$), Temkin ($R^2=0.6770$), and DKR ($R^2=0.5185$) models. This suggests that the adsorption process was heterogeneous and involved multilayers of adsorbate. Table 2 shows that

the average value of n from the Freundlich isotherm was 1.17, which is within the range of one to ten, indicating favorable adsorption. Also, the adsorption capacity can be roughly estimated by $K_f = 1.16$ (mg/g) $(mg/L)^{1/n}$.

The free energy values obtained from the D-R model for both DGPH and CGPH adsorbents were found to be lower than 8 kJ/mol (0.707 kJ/mol for DGPH and 1.581 kJ/mol for CGPH). This suggests that the adsorption process is predominantly driven by physical interactions (31).

Adsorbent kinetics

Table 3 summarizes the adsorption parameters obtained from the different kinetic models in Figures 3a-3d. The correlation coefficient (R^2) measures how well the results match the mechanism being studied. A value close to 1 means that the reaction is more consistent with it. The adsorption data showed a better agreement with the pseudo-second-order model, where the estimated values of Q_e (Est.) (2.25 and 4.57 mg/g) were very close to the observed values of Q_e (Exp) (2.25 and 4.50 mg/g) for DGPH and CGPH, respectively. This indicated that a pseudo-second-order model can better explain the adsorption kinetics of CR dye on green pea husk biosorbents.

The deviation of the intraparticle diffusion kinetic plot from the origin implies that the adsorption process is governed by multiple rate-limiting steps, such as external mass transfer, internal mass transfer, and surface reaction (43). The correlation coefficients (R^2) of 0.9443 and 0.8413 for two surfaces suggest that the intraparticle diffusion model is a reasonable representation, but not the optimal one.

Temperature effect and thermodynamic study

Figure 5 demonstrates the influence of temperature on the retention rate of CR dye on the DGPH adsorbent. According to adsorption theory, both the adsorption rate and adsorption capacity tend to increase with higher temperatures within the range of 20°C to 60°C. This observation aligns with the first law of thermodynamics, indicating that the adsorption of CR dye on DGPH is an endothermic process ($\Delta H^o > 0$). Additionally, higher temperatures facilitate faster reaction rates (35,44).

The positive values of the standard enthalpy change (ΔH^o) listed in Table 4 confirm the endothermic nature of the adsorption process. This implies that the process absorbs thermal energy from the surroundings, resulting in heat transfer into the system. The amount of heat released during physical adsorption is typically comparable to that of condensation, ranging from 2.1 to 20.9 kJ/mol, while the heat of chemisorption generally falls within the range of 80 to 200 kJ/mol (35).

In the case of DGPH, the standard enthalpy change ($\Delta H^o = 18.01$ kJ/mol) was found to be lower than 20.9 kJ/mol. This suggests that the adsorption of CR dye using DGPH is primarily attributed to a physical adsorption process rather than a chemical adsorption process.

The impact of temperature on the adsorption of CR onto CGPH was also investigated. It was observed that as the adsorption temperature increased, the CR adsorption capacity decreased, as shown in Figure 4. This suggests that CR adsorption is more favorable at lower temperatures with weaker bonding forces involved. Additionally, these findings indicate an exothermic process for CR adsorption on CGPH.

An exothermic adsorption process is typically controlled by diffusion. As the temperature increases, the mobility of dye ions tends to increase, while the interactions between the dye and CGPH active sites decrease. Moreover, at higher temperatures, there is a swelling effect within the internal structure of the adsorbent, allowing the CR dye to escape from the pores.

The determination of the standard enthalpy changes resulted in a value of -22.79 kJ/mol. The negative value indicates that the adsorption process was both exothermic and chemical in nature. Furthermore, the negative values of the Gibbs free energy changes indicate that the adsorption process was spontaneous (35,44,45).

Conclusion

This study investigated the removal of CR from aqueous solution using DGPH and CGPH as low-cost and eco-friendly adsorbents. The adsorption process was influenced by various parameters, such as contact time, pH, adsorbent dosage, initial dye concentration, and temperature. The adsorption equilibrium was achieved within 30 minutes for both adsorbents, and the optimum pH was 2. The adsorption capacity decreased with increasing adsorbent dosage and increased with increasing initial dye concentration. The Langmuir model fitted the adsorption data of DGPH better than the other models, indicating monolayer adsorption, while the Freundlich model fitted the adsorption data of CGPH better, indicating heterogeneous and multilayer adsorption. The pseudo-second-order model described the adsorption kinetics better than the other kinetic models, suggesting that the adsorption process was controlled by intraparticle diffusion. The thermodynamic analysis revealed that the adsorption of CR on DGPH was endothermic and favorable at lower temperatures, while the adsorption of CR on CGPH was exothermic and favorable at higher temperatures. The negative values of Gibbs free energy confirmed the spontaneity of the adsorption process. The study demonstrated that DGPH and CGPH could be used as effective and alternative adsorbents for the removal of CR from aqueous solution.

Acknowledgments

The authors would like to express their gratitude to the Chemistry Department of the Faculty of Science

at Misurata University for their support and resources provided during this research. The collaborative environment fostered by the Chemistry Department has been instrumental in enhancing the authors understanding and advancing their research in the field of chemistry. The authors are sincerely grateful for their contribution.

Authors' contributions

Conceptualization: Khaled Muftah Elsherif, Abdulfattah Mohammed Alkherraz.
Data curation: Basma Younus Abdulsalam Mutawia.
Formal analysis: Khaled Muftah Elsherif, Abdulfattah Mohammed Alkherraz, Basma Younus Abdulsalam Mutawia.
Funding acquisition: Abdulfattah Mohammed Alkherraz, Basma Younus Abdulsalam Mutawia.
Investigation: Basma Younus Abdulsalam Mutawia.
Methodology: Khaled Muftah Elsherif, Abdulfattah Mohammed Alkherraz.
Project administration: Khaled Muftah Elsherif, Abdulfattah Mohammed Alkherraz.
Resources: Abdulfattah Mohammed Alkherraz, Basma Younus Abdulsalam Mutawia.
Software: Khaled Muftah Elsherif, Abdulfattah Mohammed Alkherraz.
Supervision: Khaled Muftah Elsherif, Abdulfattah Mohammed Alkherraz.
Validation: Khaled Muftah Elsherif, Abdulfattah Mohammed Alkherraz, Basma Younus Abdulsalam Mutawia.
Visualization: Khaled Muftah Elsherif.
Writing–original draft: Khaled Muftah Elsherif, Howell Edwards.
Writing–review & editing: Khaled Muftah Elsherif, Howell Edwards.

Competing interests

The authors affirm that they do not have any known conflicting financial interests or personal relationships that could have influenced the findings presented in this paper.

Ethical issues

This research study adhered to the ethical guidelines and principles, ensuring the protection of human subjects, proper handling of hazardous materials, and scientific integrity. Informed consent was obtained, conflicts of interest were disclosed, and participant privacy and confidentiality were maintained. The authors are committed to upholding ethical standards in their research and reporting to contribute to knowledge advancement responsibly.

Funding

This research received no specific grant from any funding agency in the public, commercial, or not-for-profit sectors

References

1. El-Hashani A, Elsherif KM, Edbey K, Alfaqih F, Alomammy M, Alomammy S. Biosorption of Eriochrome Black T (EBT) onto waste tea powder: equilibrium and kinetic studies. To Chem J. 2018;1(3):263-75.
2. Bhoi SK. Adsorption Characteristics of Congo Red Dye onto PAC and GAC Based on S/N Ratio: A Taguchi Approach [dissertation]. Rourkela, Orissa: Department of Chemical Engineering, National Institute of Technology; 2010.
3. Imessaoudene A, Cheikh S, Hadadi A, Hamri N, Bollinger JC, Amrane A, et al. Adsorption performance of zeolite for the removal of Congo red dye: factorial design experiments, kinetic, and equilibrium studies. Separations. 2023;10(1):57. doi: 10.3390/separations10010057.
4. Elsherif KM, El-Hashani A, El-Dali A, El-Kailany R. Bi-ionic potential studies for silver thiosulphate parchment-supported membrane. Int J Adv Sci Tech Res. 2014;1(4):638-46.
5. Hua Z, Pan Y, Hong Q. Adsorption of Congo red dye in water by orange peel biochar modified with CTAB. RSC Adv. 2023;13(18):12502-8. doi: 10.1039/d3ra01444d.
6. Harja M, Buema G, Bucur D. Recent advances in removal of Congo red dye by adsorption using an industrial waste. Sci Rep. 2022;12(1):6087. doi: 10.1038/s41598-022-10093-3.
7. Khalaf IH, Al-Sudani FT, Abdul Razak AA, Aldahri T, Rohani S. Optimization of Congo red dye adsorption from wastewater by a modified commercial zeolite catalyst using response surface modeling approach. Water Sci Technol. 2021;83(6):1369-83. doi: 10.2166/wst.2021.078.
8. Elsherif KM, El-Hashani A, El-Dali A, Musa M. Ion selectivity across parchment-supported silver chloride membrane in contact with multi-valent electrolytes. Int J Anal Bioanal Chem. 2014;4(2):58-62.
9. Giwa AA, Bello IA, Oladipo MA, Aderibigbe DO. Competitive adsorption of Congo red in single and binary systems using a low-cost adsorbent. J Health Pollut. 2021;11(31):210912. doi: 10.5696/2156-9614-11.31.210912.
10. Elsherif KM, El-Dali A, Ewlad-Ahmed AM, Treban AA, Alqadhi H, Alkarewi S. Kinetics and isotherms studies of safranin adsorption onto two surfaces prepared from orange peels. Mor J Chem. 2022;10(4):639-51. doi: 10.48317/IMIST.PRSM/morjchem-v11i1.32137.
11. Vairavel P, Rampal N, Jeppu G. Adsorption of toxic Congo red dye from aqueous solution using untreated coffee husks: kinetics, equilibrium, thermodynamics and desorption study. Int J Environ Anal Chem. 2023;103(12):2789-808. doi: 10.1080/03067319.2021.1897982.
12. Elsherif KM, Yaghi MM. Studies with model membrane: the effect of temperature on membrane potential. Mor J Chem. 2017;5(1):131-8. doi: 10.48317/IMIST.PRSM/morjchem-v5i1.6324.
13. Dbik A, Bentahar S, El Khomri M, El Messaoudi N, Lacherai A. Adsorption of Congo red dye from aqueous solutions using tunics of the corm of the saffron. Mater Today Proc. 2020;22(Pt 1):134-9. doi: 10.1016/j.matpr.2019.08.148.
14. Elsherif KM, El-Dali A, Ewlad-Ahmed AM, Treban A, Alttayib I. Removal of safranin dye from aqueous solution by adsorption onto olive leaves powder. J Mater Environ Sci. 2021;12(3):418-30.

15. Nguyen TH, Dao TT, Pham GV, Do TS, Nguyen TT, Nguyen TH, et al. Effect of pH on the adsorption behaviour of Congo red dye on the Mg-Al layered double hydroxide. IOP Conf Ser Mater Sci Eng. 2020;736(2):022077. doi: 10.1088/1757-899x/736/2/022077.
16. Elsherif KM, Ewlad-Ahmed AM, Treban AA. Biosorption studies of Fe(III), Cu(II), and Co(II) from aqueous solutions by olive leaves powder. Appl J Environ Eng Sci. 2017;3(4):341-52. doi: 10.48422/IMIST.PRSM/ajees-v3i4.9806.
17. Aminu I, Gumel SM, Ahmad WA, Idris AA. Adsorption isotherms and kinetic studies of Congo-red removal from waste water using activated carbon prepared from jujube seed. Am J Anal Chem. 2020;11(1):47-59. doi: 10.4236/ajac.2020.111004.
18. Omidi Khaniabadi Y, Mohammadi MJ, Shegerd M, Sadeghi S, Saeedi S, Basiri H. Removal of Congo red dye from aqueous solutions by a low-cost adsorbent: activated carbon prepared from *Aloe vera* leaves shell. Environ Health Eng Manag. 2017;4(1):29-35. doi: 10.15171/ehem.2017.05.
19. Zarei M, Pezhhanfar S, Ahmadi Someh A. Removal of acid red 88 from wastewater by adsorption on agrobased waste material. A case study of Iranian golden *Sesamum indicum* hull. Environ Health Eng Manag. 2017;4(4):195-201. doi: 10.15171/ehem.2017.27.
20. Ounphikul B, Chantarasombat N, Hunt AJ, Ngernyen Y. A new low-cost carbon–silica composite adsorbent from a by-product of the sugar industry. Mater Today Proc. 2022;51(Pt 5):1884-7. doi: 10.1016/j.matpr.2021.10.113.
21. Rocky MM, Rahman IM, Biswas FB, Rahman S, Endo M, Wong KH, et al. Cellulose-based materials for scavenging toxic and precious metals from water and wastewater: a review. Chem Eng J. 2023;472:144677. doi: 10.1016/j.cej.2023.144677.
22. Omer AM, Dey R, Eltaweil AS, Abd El-Monaem EM, Ziora ZM. Insights into recent advances of chitosan-based adsorbents for sustainable removal of heavy metals and anions. Arab J Chem. 2022;15(2):103543. doi: 10.1016/j.arabjc.2021.103543.
23. Elsherif KM, Haider I, El-Hashani A. Adsorption of Co(II) ions from aqueous solution onto tea and coffee powder: equilibrium and kinetic studies. J Fundam Appl Sci. 2019;11(1):65-81. doi: 10.4314/jfas.v11i1.5.
24. Elsherif KM, Ewlad-Ahmed AM, Treban A. Removal of Fe(III), Cu(II), and Co(II) from aqueous solutions by orange peels powder: equilibrium study. World J Biochem Mol Biol. 2017;2(6):46-51.
25. Izadyar S, Rahimi M. Use of beech wood sawdust for adsorption of textile dyes. Pak J Biol Sci. 2007;10(2):287-93. doi: 10.3923/pjbs.2007.287.293.
26. Litefti K, Freire MS, Stitou M, González-Álvarez J. Adsorption of an anionic dye (Congo red) from aqueous solutions by pine bark. Sci Rep. 2019;9(1):16530. doi: 10.1038/s41598-019-53046-z.
27. Elsherif KM, El-Hashani A, Haider I. Biosorption of Fe(III) onto coffee and tea powder: equilibrium and kinetic study. Asian J Green Chem. 2018;2(4):380-94. doi: 10.22034/ajgc.2018.65163.
28. Alkherraz AM, Ali AK, Elsherif KM. Equilibrium and thermodynamic studies of Pb(II), Zn(II), Cu(II) and Cd(II) adsorption onto mesembryanthemum activated carbon. J Med Chem Sci. 2020;3(1):1-10. doi: 10.26655/jmchemsci.2020.1.1.
29. Alkherraz AM, Ali AK, Elsherif KM. Removal of Pb(II), Zn(II), Cu(II) and Cd(II) from aqueous solutions by adsorption onto olive branches activated carbon: equilibrium and thermodynamic studies. Chem Int. 2020;6(1):11-20. doi: 10.5281/zenodo.2579465.
30. Alkherraz AM, Elsherif KM, Blayblo NA. Safranin adsorption onto Acasia plant derived activated carbon: isotherms, thermodynamics and kinetic studies. Chem Int. 2023;9(4):134-45. doi: 10.5281/zenodo.8127687.
31. Ayawei N, Ebelegi AN, Wankasi D. Modelling and interpretation of adsorption isotherms. J Chem. 2017;2017(1):3039817. doi: 10.1155/2017/3039817.
32. Ojedokun AT, Bello OS. Kinetic modeling of liquid-phase adsorption of Congo red dye using guava leaf-based activated carbon. Appl Water Sci. 2017;7(4):1965-77. doi: 10.1007/s13201-015-0375-y.
33. Abate GY, Nguyen DT, Alene AN, Kassie DA, Addiss YA, Mintesinot SM. Cereal based traditional beverage of tella residue (attela) as a green organic pollutant sorbent for methylene blue dye removal: equilibrium, kinetics and thermodynamic studies. Indian J Chem Technol. 2023;30(2):151-64. doi: 10.56042/ijct.v30i2.64532.
34. Elsherif KM, Saad RA, Ewlad-Ahmed AM, Treban AA, Iqneebir AM. Adsorption of Cd(II) onto olive stones powder biosorbent: isotherms and kinetic studies. Adv J Chem A. 2024;7(1):59-74. doi: 10.48309/ajca.2024.415865.1415.
35. Semwal N, Mahar D, Chatti M, Dandapat A, Chandra Arya M. "Adsorptive removal of Congo red dye from its aqueous solution by Ag-Cu-CeO2 nanocomposites: adsorption kinetics, isotherms, and thermodynamics". Heliyon. 2023;9(11):e22027. doi: 10.1016/j.heliyon.2023.e22027.
36. Lafi R, Montasser I, Hafiane A. Adsorption of Congo red dye from aqueous solutions by prepared activated carbon with oxygen-containing functional groups and its regeneration. Adsorpt Sci Technol. 2019;37(1-2):160-81. doi: 10.1177/0263617418819227.
37. Omidi Khaniabadi Y, Basiri H, Nourmoradi H, Mohammadi MJ, Yari AR, Sadeghi S, et al. Adsorption of Congo red dye from aqueous solutions by montmorillonite as a low-cost adsorbent. Int J Chem React Eng. 2018;16(1):20160203. doi: 10.1515/ijcre-2016-0203.
38. de Farias RS, de Brito Buarque HL, da Cruz MR, Cardoso LM, de Aquino Gondim T, de Paulo VR. Adsorption of Congo red dye from aqueous solution onto amino-functionalized silica gel. Eng Sanit Ambient. 2018;23(6):1053-60. doi: 10.1590/s1413-41522018172982.
39. Habiba U, Siddique TA, Joo TC, Salleh A, Ang BC, Afifi AM. Synthesis of chitosan/polyvinyl alcohol/zeolite composite for removal of methyl orange, Congo red and chromium(VI) by flocculation/adsorption. Carbohydr Polym. 2017;157:1568-1576. doi:10.1016/j.carbpol.2016.11.037.
40. Wanyonyi WC, Onyari JM, Shiundu PM. Adsorption of Congo red dye from aqueous solutions using roots of *Eichhornia crassipes*: kinetic and equilibrium studies. Energy Procedia. 2014;50:862-9. doi: 10.1016/j.egypro.2014.06.105.
41. Alkherraza AM, Elsherifb KM, El-Dalib A, Blaybloa NA, Sasic M. Thermodynamic, equilibrium, and kinetic studies of safranin adsorption onto *Carpobrotus edulis*. Asian J Nanosci Mater. 2022;5(2):118-31. doi: 10.26655/ajnanomat.2022.2.4.
42. Bayramoglu G, Arica MY. Adsorption of Congo red

dye by native amine and carboxyl modified biomass of *Funalia trogii*: isotherms, kinetics and thermodynamics mechanisms. Korean J Chem Eng. 2018;35(6):1303-11. doi: 10.1007/s11814-018-0033-9.

43. Dada AO, Ojediran JO, Okunola AA, Dada FE, Lawal AI, Olalekan AP, et al. Modeling of biosorption of Pb(II) and Zn(II) ions onto PAMRH: Langmuir, Freundlich, Temkin, Dubinin-Raduskevich, Jovanovic, Flory-Huggins, Fowler-Guggenheim and Kiselev comparative isotherm studies. Int J Mech Eng Technol. 2019;10(2):1048-58.
44. Ahmadi S, Rahdar S, Igwegbe CA, Rahdar A, Shafighi N, Sadeghfar F. Data on the removal of fluoride from aqueous solutions using synthesized P/γ-Fe2O3 nanoparticles: a novel adsorbent. MethodsX. 2019;6:98-106. doi: 10.1016/j.mex.2018.12.009.
45. Etemadinia T, Allahrasani A, Barikbin B. ZnFe2O4@SiO2@Tragacanth gum nanocomposite: synthesis and its application for the removal of methylene blue dye from aqueous solution. Polym Bull. 2019;76(12):6089-109. doi: 10.1007/s00289-019-02681-7.